

MATCHED TIME-FREQUENCY REPRESENTATIONS AND WARPING OPERATOR FOR MODAL FILTERING

Grégoire Le Touzé, Jérôme Mars, and Jean-Louis Lacoume

Laboratoire des Images et des Signaux
INPG/ENSIEG, Grenoble, France
email: gregoire.letouze@lis.inpg.fr

ABSTRACT

In waveguide, pressure signals break up into modes. This paper exposes two signal processing tools to realise a mode filtering adapted to guided waves. The first one is a time-frequency representation invertible on which filtering is possible. The second is an axe warping operator. We test both methods on real data and compare performances on synthetic dataset. We finally show that these two tools supplement each other.

1 Introduction

In Underwater Acoustics, research of geoacoustical parameters and source localization (source depth, source-sensor distance) are very large fields of prospects. In the classical environment of shallow water, waveguide is taken as a model of the oceanic medium. Starting from long range, pressure signal (resulting from an impulse source) breaks up into modes due to the dispersive propagation in the waveguide.

The mode's characteristics (energy, phase, time-frequency evolution...) contain crucial information about environment parameters and source localization. We can filter them with a vertical array thanks to their vertical orthogonality [1] and with a horizontal array thanks to the frequency-wavenumber transform [2]. Our aim is to obtain the same information with a single sensor. For pressure wideband signals, modes are following dispersion curves in the time-frequency ($t - f$) plane. The objective of this study is to give tools to filter modes issued from single sensor analysis. Because they are dispersive, modes constitute multiple non-linear structures in the time-frequency plane. We are thus in a complex situation for t-f representation and filtering.

We first briefly present waveguide and mode dispersion in section 2. Based on previous works [3], we have already developed [4] time-frequency representations (TFR) matched to the shallow water propagation. This TFR is invertible and allows a mode filtering processing. Its principles are presented on the section 3. We want now to focus on a new tool to avoid the non-linearity problem. Starting from the theoretical dispersive relationship, we can build an axe warping operator [5] and use unitary equivalence principle [6]. This method, its applications and its conditions for mode filtering and time-frequency localization improvement are exposed in section 4. We then apply both methods on real dataset and compare them on synthetic dataset in section 5.

2 Waveguide configuration

In shallow water environment, waveguide is a common model. The simplest model is called perfect waveguide and only takes into account the water layer.

Geoacoustic parameters (number of layers, depths, propagation velocities, densities) associated with modes theory establish relationship between group velocity and frequency for each integer mode m . In addition, with knowledge of the source-sensor distance R , the energy distribution of mode in the time-frequency plane can be deduced [8]. This energy follows a non-linear dispersive curve:

$$v = u_m(\tau) \quad (1)$$

For the perfect waveguide, eq. 1 is:

$$v = \frac{(2m-1)C_1^2 \tau}{4D[(C_1 \tau)^2 - R^2]^{1/2}} \quad (2)$$

for the m^{th} mode and where C_1 is the velocity in the water layer, D the depth guide and R the source-sensor distance (figure 1).

3 Matched Time-Frequency representations

The first tool developed [4] is time-frequency representations allowing mode filtering. They respect the two objectives:

- Separate modes in the time-frequency plane;
- Be invertible for mode filtering.

By using a TFR, we are limited by the Heisenberg-Gabor inequality. We must circumvent the time-frequency uncertainty and avoid interferences between components. TFR built are matched to the waveguide model of propagation and consist in projecting the signal on an atom dictionary tiling the $t - f$ plane. Atoms are defined by:

$$h_{\tau, \xi}(t) = h_{\tau}(t) e^{j \xi m(t)} \quad (3)$$

where the modulation rate $\xi m(t)$ is calculated starting from the theoretical dispersion relation 1. To cover all the time-frequency plane, we calculated the mode number m' for each point of the plane by inversion of the dispersion relation. m' is no more necessarily an integer: we have a *continuum* of m . As a result, the atoms of projection differ from a place to other in the time-frequency plane (figure 2). Module $h_{\tau}(t)$ is calculated so that the continuous dictionary $\{h_{\tau, \xi}(t); \tau \in D_f \text{ and } \xi \in \mathbb{R}\}$ (with D_f the time domain definition) constitute a base (respecting the "closing

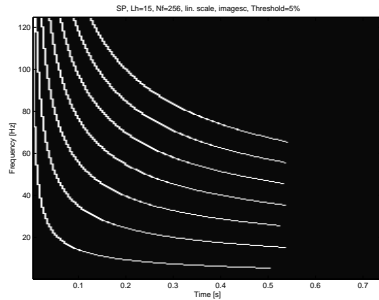


Figure 1: 7 first modal curves in the time-frequency plane (with North Sea survey configuration)

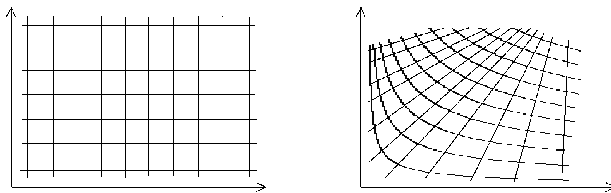


Figure 2: Paving of the time-frequency plane by projection atoms for Short Time Fourier Transform (left) and for matched TFR (right)

condition" [9]). Figure 2 shows that atoms are following modal curves. Taking a large window, TFR is not precise along the curve but precise perpendicularly to them. Time-frequency localization is thus not relevant but modes are well separated. Chen *et al.* [3] have developed this matched TFR for the perfect waveguide. We completed it to make the TFR invertible, we adapted it to an approximation of the more realistic Pekeris waveguide [7] and generalised the methodology in [4].

Mode filtering is then allowed and facilitated by these matched (and invertible) TFR thanks to the better separation of modes in the time-frequency plane. To realise mode filtering, we use the classical image segmentation Watershed algorithm [10] on the TFR. After segmentation, we select the wanted mode and invert the TFR. We have consecutively the time version of modes, we can thus reach phase and amplitude. We can also reach a more precise shape of the mode in the time-frequency plane because no more interferences with others modes are present.

4 Axe Warping Operator

To avoid problems due to non-linear time-frequency structures, we propose to use a classical unitary operator [5]: the axes warping operator. It is defined for a signal $x(\tau)$ as an operator \mathbf{W} on $L^2(\mathbb{R})$ whose effect is given by:

$$(\mathbf{W}x)(t) = |w'(t)|x[w(t)] \quad (4)$$

where $w(t)$ is a smooth, one-to-one function. Starting from the theoretical modulation formulation of modes function $\xi(\tau)$, we want to design the warping function. This function transforms non-linear modes on time domain τ , on linear component on warped time domain t . Once

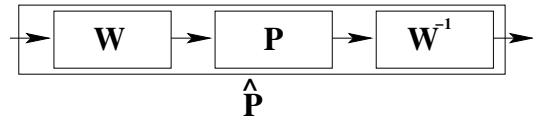


Figure 3: Schema of unitary equivalence principle

this transformation carried out, we can use the concept of Unitary equivalence developed in [6]. By definition, two operators $\hat{\mathbf{P}}$ and \mathbf{P} are unitary equivalent if $\hat{\mathbf{P}} = \mathbf{W}^{-1}\mathbf{P}\mathbf{W}$ where \mathbf{W} is a unitary transform. This principle is illustrated on figure 3. A conventional system of signal processing \mathbf{P} (linear filter, time-frequency representation...) is placed between two unitary transforms \mathbf{W} and \mathbf{W}^{-1} .

Choosing the well matched operator \mathbf{W} allows two possibilities:

- 1/ As modes are separable in frequency, we can make a mode filtering designed by \mathbf{P} (band-pass filter).
- 2/ As modes are linear in the time-frequency plane, there is no more the non-linear time-frequency representation limitations. We can so apply a time-frequency representation \mathbf{P} with an accuracy time-frequency localization.

4.1 Axe Warping matched to perfect waveguide

The instantaneous frequency is the derivate of the instantaneous phase. For the perfect waveguide, we start from the dispersive relation (eq. 2):

$$\xi_m(\tau) = 2\pi \int v_m(\tau) d\tau = 2\pi(2m-1) \left(\frac{(C_1\tau)^2 - R^2}{4D} \right)^{1/2} \quad (5)$$

The pressure signal which is a sum of modes is:

$$p(\tau) = \sum_m A_m e^{j\xi_m(\tau)} \quad (6)$$

where A_m is the mode amplitude. Starting from this law, the warping operator is described by:

$$(\mathbf{W}p)(t) = |w'(t)| \sum_m A_m e^{j\xi_m(w(t))} \quad (7)$$

To fit n^{th} mode on pure frequency f_w in the warped domain, following condition $\xi_n(w(t)) = f_w t$ is necessary. We then deduce:

$$w(t) = \frac{(k^2 t^2 + R^2)^{1/2}}{C_1} \quad (8)$$

with $k = f_w D / 4(2m-1)$.

The pressure signal studied is multi-components. The warping operator can shift all the structures to pure frequencies in the warped space if they are homogeneous. This is the case for modes in the perfect waveguide as they are linked to each other by a factor dilation m . By integrating this coefficient on $w(t)$, we can use the same warping operator to filter all the modes. Because they are strictly separated in the warped frequency domain, we can use a perfect band-pass filter $\hat{\mathbf{F}}$. $\hat{\mathbf{F}}$ corresponds to the \mathbf{P} operator (figure 3). Unitary equivalence allows the modal filtering on applying $\hat{\mathbf{F}} = \mathbf{W}^{-1}\mathbf{F}\mathbf{W}$ with \mathbf{W} and \mathbf{W}^{-1} constructed *via* $w(t)$ and $w^{-1}(t)$ function

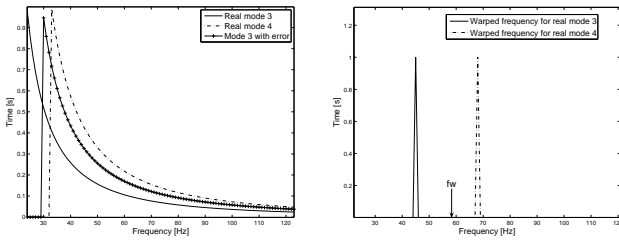


Figure 4: Left: Modal curve layout for real mode 3, 4 and mode 3 with an error on D of 20%. Right: Corresponding frequency on the warped frequency domain. f_w represents the theoretical warped frequency of the mode 3 with erroneous parameter

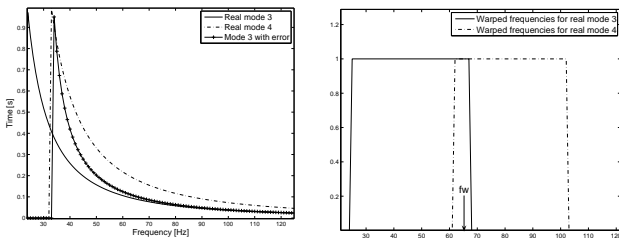


Figure 5: Left: Modal curve layout for real mode 3, 4 and mode 3 with an error on R of 50% and C_1 of 100%. Right: Corresponding frequencies on the warped frequency domain. f_w represents the theoretical warped frequency of the mode 3 with erroneous parameters

following eq. 7 and 8. With this method we are free from the problem of time-frequency uncertainty which remains (although circumvented) in matched TFR.

Mode filtering with axes warping method have to two main limitations:

- Adequacy of the real waveguide with the perfect model;
- Accuracy knowledge of parameters (source-sensor distance R , waveguide depth D , velocity C_1 ...)

Both of these limitations can cause a spreading out of the warping mode localization. Instead of being located on a pure frequency f_w , the warped mode will be located around this frequency or frequency shifted. To evaluate this shift or spreading out, we can compare the real modal dispersion (eq. 1) with that integrated to the warping operator (with error on parameters and eventually non appropriate model). If those curve are "parallel", there is a simple dilation factor between them. Consecutively, modal frequency will be shifted in the warped frequency but not spread out: the mode filtering is still possible but not at the theoretical frequency f_w . It is the case for an error on the waveguide depth D (figure 4). If we have an significant error on R or C_1 , warped modal frequency will be shifted and spread out: mode filtering becomes impossible (figure 5).

4.2 Time-Frequency accuracy localization

A second application of this method is to improve the time-frequency localization accuracy of modes. In practical situations, time-frequency localization of a mode is

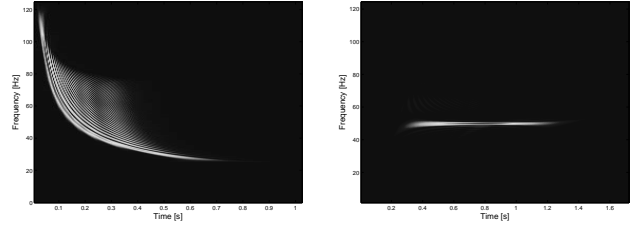


Figure 6: Left: Wigner-Ville distribution for filtered mode 3. Right: Wigner-Ville distribution for filtered mode 3 on warped domain.

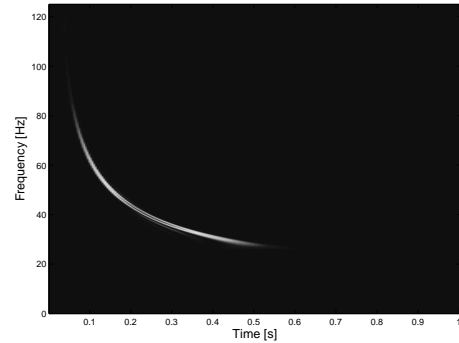


Figure 7: Warping Wigner-Ville Operator application on filtered mode 3

correlated with source-sensor distance R [12]. Classical methods (spectrogram, reassigned spectrogram, Wigner-Ville distribution...) are not efficient to characterize multiple non-linear structures. In warped domain, structures are linear, spectrogram or reassigned spectrogram are thus matched. In case of a single linear filtered structure we can apply the perfect time-frequency method localization for single linear structure: the Wigner-Ville distribution.

The protocol applied to the pressure signal to have the better time-frequency localization is defined as: $\hat{F} = \mathbf{W}^{-1} \mathbf{F} \mathbf{W}$ for filtering and then applying the Wigner-Ville warping operator $\hat{\mathbf{W}} \mathbf{V} = \mathbf{W}^{-1} \mathbf{W} \mathbf{V}(\hat{F}) \mathbf{W}$. Example of Wigner-Ville distribution on mode 3 is given figure 6 and 7: filtering remove interferences between modes and Wigner-Ville warping operator interferences intra mode.

5 Comparison between the two methods

5.1 Results on Real data

Real case results from a survey in North Sea for which the source-sensor distance $R = 5000\text{m}$. Theoretical curves of the first 7 modes are presented figure 1. Time version of the pres-

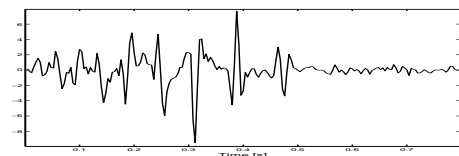


Figure 8: Pressure signal for $R=5000\text{m}$ (North Sea)

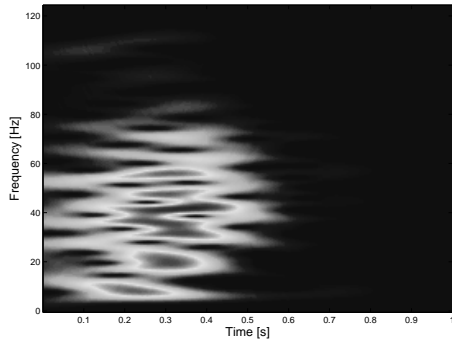


Figure 9: Module of Short Time Fourier Transform for R=5000m (North Sea)

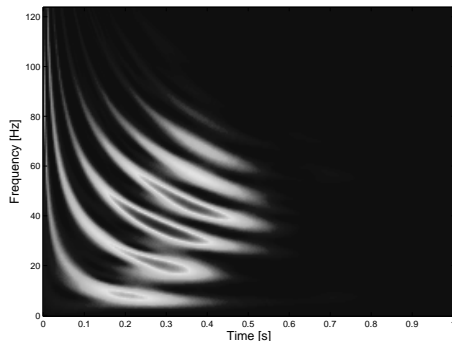


Figure 10: Matched TFR for R=5000m (North Sea)

sure signal is shown figure 8. The matched TFR is presented figure 10 and the Short Time Fourier Transform [11] figure 9. Benefit given by matched TFR with respect to the traditional methods can clearly be seen: for the classical methods, time-frequency compromise doesn't make possible to distinguish modes which is the case with matched TFR. Mode filtering is then possible. To illustrate the warping method, we plot the spectrum of the original signal (figure 11) and those of the warped signal (figure 12). Once again, mode filtering is possible with this method: 7th first modes are clearly separated in the warped domain which is not the case in the original domain (we distinguish peaks but not necessarily linked to a mode).

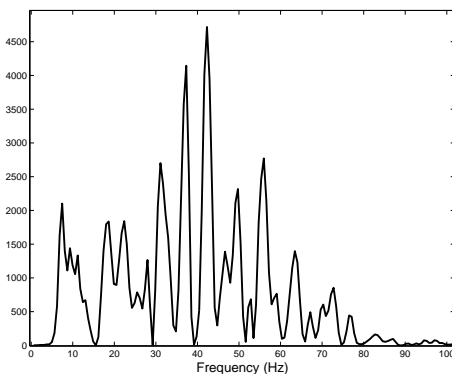


Figure 11: Spectrum of the signal for R=5000m (North Sea)

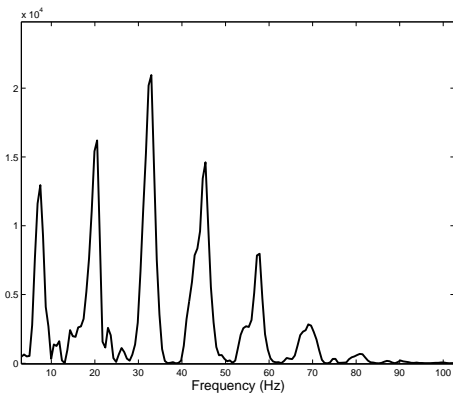


Figure 12: Spectrum of the warped signal for R=5000m (North Sea)

5.2 Modal filtering performances comparison

5.2.1 Without errors

Energies of the modes inform us about the source depth z_s [2], their phase and their time-frequency localization about the distance R [12]. Modes can also be used to extract geoacoustical parameters [12]. We propose to evaluate the mode restitution in time measuring the absolute mean error on n samples:

$$E = \frac{100 \sum_{i=1}^n |x(i) - \hat{x}(i)|}{\sum_{i=1}^n |x(i)|} \quad (9)$$

with x the original mode and \hat{x} the filtered mode. The error is calculated for different values of R (from $R=2500m$ to $R=25000m$) with the configuration of the real North Sea dataset presented in the previous section. The model of simulation is based on Pekeris waveguide (more realistic than the perfect one).

This evaluation is made with the matched TFR (section 3), with the axe warping method (section 4) and with the STFT. In this last case, we use the same protocol than with the matched TFR. With the STFT, mode are not separable less $R=20000m$ because of the STFT limitations. For this method, the evaluation begins thus in this value of R . Results are presented figure 13. As we can see, mode filtering with warping operator is more efficient than with the matched TFR. Indeed, with the warping operator, we have no more problem with time-frequency uncertainty whereas it is still a problem for the matched TFR even if it is circumvented along the modal curve. Performances of warping are thus higher. Starting from a sufficient long distance R , performance converge towards mode filtering by STFT. Modes are then more separable but the spreading out of energy in time prevents a good filtering (performances are lower).

5.2.2 With errors

We apply now significant errors on the knowledge of parameters: starting with the same signals, we apply methods considering that $R' = R/2$ and $C'_1 = 2C_1$. Because we have seen that error on D doesn't affect the accuracy of filtering, we don't apply an error on the depth.

Results are presented figure 14. If performances of filtering

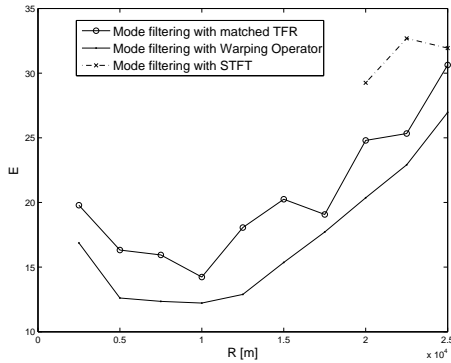


Figure 13: Error E of restitution with the 3 methods

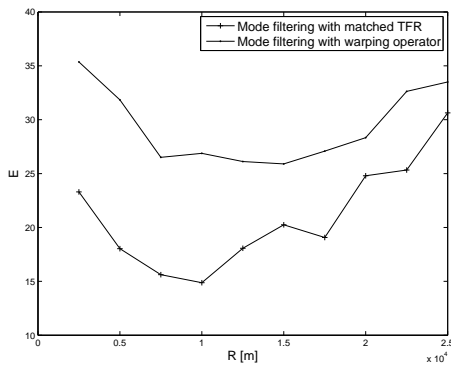


Figure 14: Error E of restitution with errors on parameters knowledge

via matched TFR are not significantly changed, it is not the case for warping method. Error on C_1 or R must *a priori* affect both filtering methods. But as we are projecting signal locally (on atoms) on a *continuum* of m' values, matched TFR allows a high robustness (differences are always locally small). As a result, on the one hand matched TFR are not sensitive to badly estimated parameters, on the other hand, warping method which apply a global law (not recalculated locally) is not matched to this type of badly estimated situation.

6 Conclusion

We propose in this paper two signal processing tools to filter modes in a shallow water environment. One is a time-frequency representation matched to the model of propagation. We project the pressure signal on dictionary atoms locally defined. Modes are well separated on the TFR and can be filtered using a Watershed algorithm. The second is the application of an axe warping operator which transform non-linear structures (the modes) on linear structures in the warped domain. Modes are well separated in the frequency domain and we can filter them with classical band-pass filtering.

Performances evaluation show that the filtering with matched TFR is less efficient when parameters are well estimated but more on the contrary case. This 2 tools thus supplement each other: on an filtering application, we can imagine using the TFR for a first parameters estimation and the warping

method for refining the filtering and the parameters evaluation.

REFERENCES

- [1] E.C. Shang, "Source depth estimation in waveguides," *J.Acoust.Soc.Am*, vol. 77, pp. 1413–418 1985.
- [2] B. Nicolas J. Mars and J-L. Lacoume, "Source depth estimation using modal decomposition and frequency-wavenumber transform," in *Proc. EUSIPCO 2004*, Vienna, 2004.
- [3] C-S. Chen J.H. Miller G.F Bourdeaux-Bartels G.R. Potty and C.J. Lazauski, "Time-frequency representations for wideband acoustic signals in shallow water," in *Oceans 2003 Proceedings*, vol. 5, pp. SP2903–SP2907, 2003.
- [4] G. Le Touzé B. Nicolas J. Mars J-L. Lacoume and D. Fattaccioli "Représentations temps-fréquence adaptées aux ondes guides," in *GRETSI 2005*, Louvain-La-Neuve, Belgium, 2005.
- [5] A.E. Taylor, *Functional Analysis*, Wiley Editor, 1958.
- [6] R.G. Baraniuk, "Unitary Equivalence : a new twist on signal processing," *IEEE Trans. on Acoust. Sig. Proc.*, vol. 43(10), pp. 1226–1234, 1995.
- [7] C.L. Pekeris, "Theory of propagation of explosive sound in shallow water," *Geol.Soc.Am.Mem*, 1947.
- [8] L. Tolstoy and C.S. Clay, *Ocean Acoustics : Theory and Experiment in Underwater Sound*, American Institute of Physics, 1987.
- [9] P. Flandrin, *Temps-fréquence*, HERMES, 1993.
- [10] L. Vincent P. Soille, "Efficient Algorithm Based on Immersion Simulations," *IEEE Trans. on Pattern Analysis and Machine Intelligence*, vol. 13(6), pp. 583–598, 1991.
- [11] J.B. Allen and L.R. Rabiner, "A unified approach to Short Time Fourier Analysis and Synthesis," *Proc. IEEE*, vol. 65(11), pp. 1558–1564, 1977.
- [12] G.R. Potty J.H. Miller and J.F. Lynch, "Inversion for sediment geoacoustical properties at New England Bight," *J.Acoust.Soc.Am*, vol. 114(4), pp. 1874–1887, 2003.